Proceedings of the 28th IEEE
EMBS Annual International Conference
New York City, USA, Aug 30-Sept 3, 2006

Optical Mapping System for Visualizing Arrhythmias in Isolated Mouse Atria

Robyn Schmidt and Anders Nygren, *Members, IEEE*

Abstract— **Optical mapping has become an important technique in the study of cardiac electrophysiology, especially in terms of investigating the mechanisms of cardiac arrhythmias. The increasing availability of transgenic mice as models for cardiovascular disease is driving the need for instrumentation suitable for the study of electrical activity in the mouse heart. In this paper we evaluate our optical mapping system's ability to clearly record induced arrhythmic activity in an isolated mouse atrial preparation. Preliminary results indicate that the signal quality is high enough that individual optically recorded action potentials can be discerned in many pixels, even without post-processing for noise removal. The optical mapping video is clear enough for general observations regarding the patterns of electrical propagation during arrhythmic behaviour. The induced arrhythmias appear to have a regular pattern of activity, and are likely best classified as atrial tachycardias.**

I. INTRODUCTION

Atrial fibrillation (AF) is the most common sustained cardiac arrhythmia, with an estimated 2.2 million people affected in the United States [1]. AF is foremost a disease of the elderly - going from a prevalence of 0.5% for people in their 50s up to 10% for those aged 80 and above [2]. AF continues to be an important health concern, with a mortality of 77,800 in the United States with atrial fibrillation or atrial flutter listed as an underlying or contributing cause of death [1]. All of these factors are driving the need to improve our understanding of the mechanisms surrounding atrial rhythm disturbances.

Optical mapping [3] has become an important technique in the study of cardiac electrophysiology because it provides a recording of the time course of electrical activity (action potentials) across the spatial extent of the tissue. Optical mapping has been successful at increasing our knowledge of atrial arrhythmic activity using a variety of animal models such as sheep [4], dogs [5], and in both wild type [6] and transgenic mice [7].

The mouse as a model for cardiac arrhythmias has many benefits stemming from extensive work in the development of transgenic animals to model a wide variety of cardiac disease. However, the mouse heart presents many challenges due to its extremely small size. Despite these difficulties, there has been successful work at inducing atrial arrhythmias in the mouse [6], [7]. However, in terms of optical mapping studies, the physical geometry of a whole-heart preparation makes it difficult to record images across the entire atria without a complex imaging setup (e.g. by using multiple cameras as in [4]), or without sacrificing spatial resolution and focusing only on a particular region of the atria. One of the main benefits of our isolated atrial preparation is that the tissue is pinned out flat, such that the entire posterior wall and both atrial appendages can be imaged with a relatively simple optical mapping setup. Previous work has shown the feasibility of using this isolated atrial preparation for the study of baseline electrophysiology parameters in the mouse heart [8]. The goal of this work is to investigate our optical mapping system's ability to record induced arrhythmias in the isolated mouse atrial preparation.

II. METHODS

A. Atrial Preparation

Atrial preparations were isolated from 6- to 8-week-old male C57BLK6 mice as described previously [8]. All methods complied with the National Institutes of Health *Guide for the Care and Use of Laboratory Animals* (NIH Publication No. 85-23, Revised 1996) and with University of Calgary guidelines. Briefly, mice were anesthetized via isoflurane inhalation and sacrificed by cervical dislocation. The heart was quickly excised and placed in a superfusion dish. The tissue was continually superfused at a flow rate of 3 ml/min and at a temperature of 35±1°C with Krebs solution of the following composition (in mM): NaCl 118.0, KCl 4.7, KH_2PO_4 1.2, $MgSO_4$ 1.2, $CaCl_2$ 1.0, $NaHCO_3$ 25.0, Glucose 11.1. The superfusion solution was bubbled with 95% O_2/5% CO_2 in a 37°C water bath to maintain a pH of 7.4. The isolation procedure was carried out with the tissue in the superfusion solution, and involved dissecting away the ventricular tissue to leave a preparation consisting only of the interconnected atria. The isolated atrial preparation was then pinned to the sylgard coating at the bottom of the superfusion dish. A unipolar Ag/AgCl recording electrode was placed at each atrial appendage for electrogram recordings, and a stainless steel pacing electrode was placed near the inferior vena cava. After a 20-minute settling period, ryanodine (200 nM) was added to the superfusate. The administration of ryanodine depletes the sarcoplasmic reticulum Ca^{2+} stores, resulting in reduced contraction force and the suppression of motion artifacts in the optical mapping recordings. The preparation was stained with the voltage-sensitive dye di-4-ANEPPS (10 μM) for 10 minutes before starting the optical mapping recordings.

This research was supported by a Grant-in-Aid from the Heart & Stroke Foundation of Canada and the University of Calgary

R. Schmidt is with the Department of Electrical and Computer Engineering, Schulich School of Engineering, University of Calgary, 2500 University Dr NW, Calgary AB T2N 1N4, Canada, schmidtr@ucalgary.ca

A. Nygren is with the Centre for Bioengineering Research and Education and the Department of Electrical and Computer Engineering, Schulich School of Engineering, University of Calgary, 2500 University Dr NW, Calgary AB T2N 1N4, Canada, nygren@ucalgary.ca

B. Imaging System

The optical mapping system has been described previously [8]. Briefly, the illumination light is provided by a 250 W quartz tungsten halogen lamp and is bandpass filtered at 500±25 nm. The emitted fluorescence signal is filtered by a longpass Schott glass filter at 590 nm, and is recorded by a CCD camera (Dalsa CA-D1-0128T) with a field of view of 10x10 mm and a frame rate of 950 Hz.

Minor changes to the imaging system were implemented to maximize the illumination light intensity arriving at the tissue, in an effort to increase the quality of the optical data. These optimizations included a new dichroic mirror (better suited to the size of the preparation), a shutter with larger aperture and adjustments to the overall length of the light path. With these modifications, it is possible to achieve an illumination intensity of 50-60 mW/cm^2 at the surface of the perfusion dish, representing a 2-3-fold increase in illumination intensity compared to previous recordings [8].

C. Data Processing

The recorded images were processed using custom software written in IDL and C++. Each pixel was processed as follows: 1) subtraction of the background fluorescence 2) linear trend removal and 3) sign reversal, such that a depolarization corresponds to a positive signal. In the case of arrhythmia recordings, no further processing for noise removal was applied. In the case of sinus or paced recordings, the data were signal averaged over 10 s to improve the signal-to-noise ratio, using either the peak of the electrogram (for sinus recordings) or the stimulus signal (for paced recordings) as the time reference.

D. Stimulation Protocol

Initial baseline recordings were performed with the heart in sinus rhythm and also while being paced at a rate slightly more rapid than the sinus rate. The pacing was achieved via a unipolar electrode placed near the inferior vena cava. Stimuli were of 2 ms duration, at twice the threshold current. After the initial baseline recordings, a rapid burst pacing protocol was applied to attempt arrhythmia induction. For the burst pacing protocols, the cycle length of the stimulus pulse train was decreased to a minimum of 10 ms. The burst pulses were delivered for up to 4 s and then abruptly terminated. After the initial arrhythmia induction attempts, the I_{KACh} (muscarinic receptor) agonist carbachol (CCh, 10 μM) was added to the superfusion solution, and the burst pacing protocols were repeated to evaluate arrhythmia induction success under cholinergic stimulation.

The initial arrhythmia induction attempts via burst pacing were not recorded with the imaging system, in order to avoid photobleaching effects and tissue damage which may result from excessive exposure to the illumination light [9]. The imaging system is not required to determine the success or failure of arrhythmia induction, as this can be determined simply by observing the electrogram. However, once a successful set of parameters for arrhythmia induction was found (i.e. stimulation frequency and number of bursts), repeat trials were performed to re-induce the arrhythmia and record the arrhythmic activity with the optical mapping system.

III. RESULTS

A. Cholinergic Stimulation

As reported previously, the administration of carbachol (CCh, 10 μM) reduces the action potential durations (APDs) in the isolated atrial preparation [8]. Administration of CCh also causes a drastic slowing in the sinus rate of the isolated atrial preparation, and often the sinus rhythm stops altogether. Fig. 1 illustrates a typical example of the APD reduction in a single pixel (corresponding to an area of 167x167 μm) in each of the right and left atrial appendages. In order to clearly show the APDs, the data in Fig. 1 has been averaged over 10 s using the stimulus pulse as the time reference. Fig. 2-B highlights the slowed sinus conduction after cholinergic stimulation.

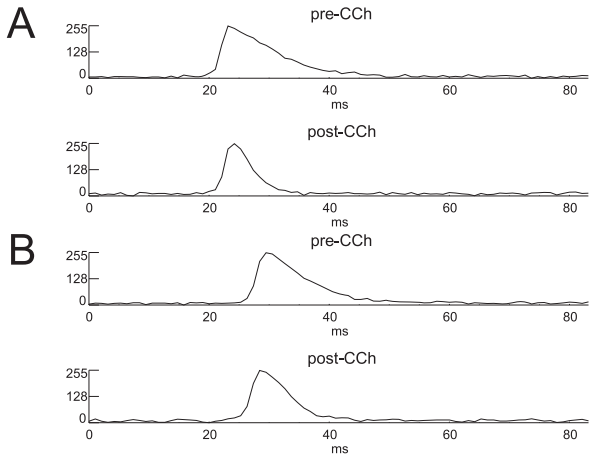

Fig. 1. Results showing the shortening of action potential duration (APD) after administration of carbachol (CCh, 10 μM). Each time series consists of an averaged signal taken over 10 s, with the heart paced at 100 ms (normal sinus rate was approximately 128 ms). **A:** Typical APD reduction in a single right atrial appendage pixel. **B:** Typical APD reduction in a single left atrial appendage pixel.

B. Arrhythmia Induction

Our initial results show that arrhythmia induction via a burst pacing protocol is feasible in the isolated mouse atrial preparation after cholinergic stimulation. Fig. 2 illustrates a typical arrhythmia induction. Each panel in Fig. 2 illustrates a single optically recorded action potential from a pixel in each of the right and left atrial appendages, as well as the recorded electrogram. The illustrated arrhythmia was introduced after delivering a burst train consisting of 9 pulses at a cycle length of 10 ms. In the given preparation, this stimulation protocol was unsuccessful in inducing arrhythmias prior to the administration of CCh (15 trials), but was successful in inducing an arrhythmia in 9 out of 15 trials after cholinergic stimulation. All induced arrhythmias terminated spontaneously within 5 seconds.

Fig. 3 shows three subsequent frames for each of the right and left atrial appendages from the same induced arrhythmia

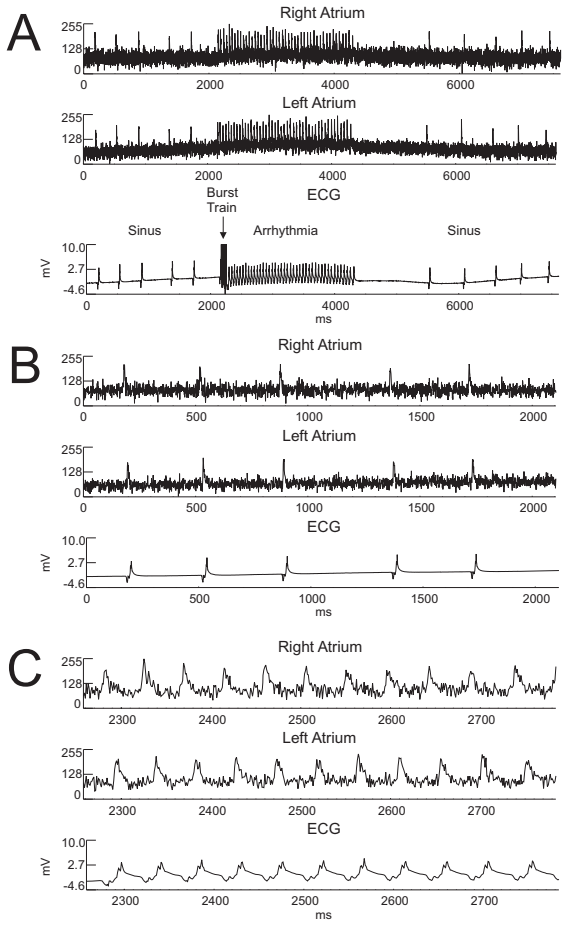

Fig. 2. Example of an induced tachyarrhythmia in isolated mouse atria. In each panel, a relatively noise-free pixel (time series) from each of the right and left atrial appendages is shown along with the electrogram (ECG). **A:** Illustration of the slowed sinus rate (due to CCh), the short burst train (9 bursts, 10 ms apart), the induced tachyarrhythmia, spontaneous arrhythmia termination and subsequent return to slowed sinus conduction. **B:** Detail of the slowed sinus conduction. **C:** Detail of the induced tachyarrhythmia.

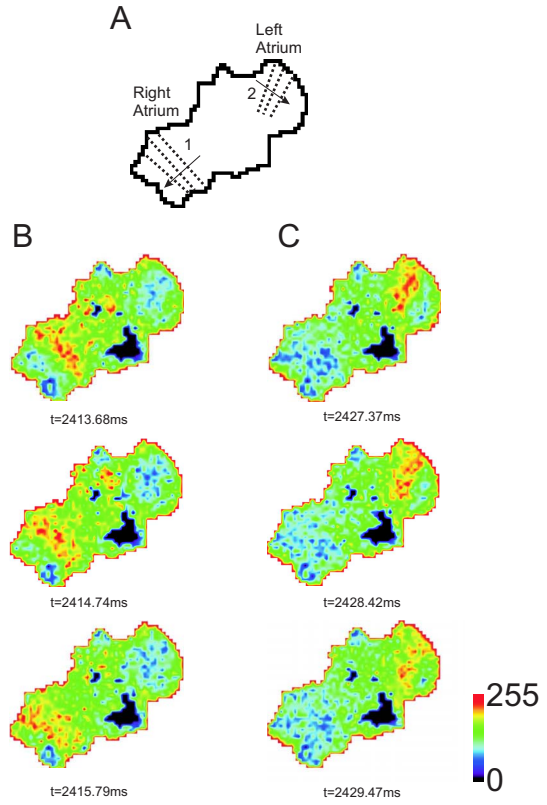

Fig. 3. Illustration of the planar wavefront of activity during the induced arrhythmia for three subsequent frames in both the right and left atria. In all panels the right atrium is on the left-hand side. **A:** Summary of the propagation of electrical activity. The dashed lines are approximations to the wavefronts illustrated in **B** and **C**. The activity first propagates in a planar wavefront across the right atrial appendage (1). After a delay, the activity propagates across the left atrial appendage (2). **B:** Three optically recorded frames illustrating the wavefront of activity as it moves across the right atrial appendage. The red area indicates action potential maxima and translates into the activation wavefront as it moves across the tissue. **C:** Three optically recorded frames illustrating the wavefront of activation propagating across the left atrium.

shown in Fig. 2. Here, the signal quality is relatively high, and the wavefronts of electrical activation (corresponding to the areas in red) can be detected in each atrial appendage. The wavefront during the induced arrhythmia propagates in a pattern similar to that seen in sinus rhythm. The activity starts near the sulcus terminalis, and travels towards the edge of the right atrial appendage. After a delay, the wavefront of activation can be seen in the left atrium, and again travels from the inter-atrial area towards the appendage. In the induced arrhythmias there was always a 1:1 correspondence between right and left activation, indicating that both atria remain synchronized during the arrhythmic activity. These observations support the conclusion that the arrhythmias are better classified as organized tachycardias rather than disorganized fibrillation.

IV. DISCUSSION

The successful induction of arrhythmias in the isolated mouse atrial preparation appears to rely on cholinergic stimulation, consistent with previous work in the mouse [6], [7], and in larger species such as the dog [10]. Cholinergic stimulation facilitates arrhythmia induction due to a decrease in atrial refractoriness which favors the development of re-entrant circuits. After the administration of CCh, the action potential durations (APDs) in the mouse atria are shortened. This in turn reduces the wavelength (APD$\times$conduction velocity), which is a critical parameter in establishing and maintaining re-entrant arrhythmic activity. In order to sustain re-entry, the wavelength must be shorter than the re-entrant path length. This ensures that when a wavefront of activation returns to its starting point, that area of tissue is no longer refractory and can be re-excited, such that the re-entrant pattern of activity can continue indefinitely. If the opposite were true (and the wavelength was longer than the potential re-entrant path length), then the wavefront of activation, upon returning to its starting point, would meet refractory tissue and die out. Consequently, the shortening of APD due to CCh may facilitate re-entrant arrhythmias by allowing for smaller path lengths (compared to the pre-CCh case) which can sustain the re-entrant activity.

The arrhythmia illustrated in Fig. 2-C appears to be very regular and lacks the characteristic disorganization of atrial fibrillation. Consequently, this arrhythmia is likely most accurately described as an atrial tachyarrhythmia rather than atrial fibrillation. In other words, the underlying mechanism of the arrhythmia is likely a stable single re-entrant circuit. Tachyarrhythmias are still interesting in the study of atrial arrhythmias since they can easily break down into fibrillatory behaviour. Furthermore, sustained atrial tachycardias have been shown to be responsible for the same type of electrical remodelling that occurs in the presence of atrial fibrillation. This remodelling involves Ca^{2+} loading effects, which cause the cell to respond with a decrease in the L-type Ca^{2+} current (I_{CaL}). This decrease in (I_{CaL}) causes a decrease in the APD which in turn may support the induction or maintenance of fibrillatory rhythms [2].

The signal-to-noise ratio (SNR) in the optical mapping data is high enough that individual action potentials in some pixels can readily be identified without any post-processing for noise removal, as shown in Fig. 2. CCD camera noise and SNR at various light intensities can be characterized by a photon transfer curve [11], which has been done previously with a camera similar to the one in our system [12]. In mid-to-high illumination levels (including levels typical in our experimental setting), photon shot noise dominates and the total noise level for the CCD array is approximately $\sqrt{n}$ for an illumination level corresponding to n incident photoelectrons. This results in $SNR = \frac{n}{\sqrt{n}} = \sqrt{n}$ [11]. Clearly, increasing the signal intensity will improve the SNR. Qualitatively, we have observed a substantial improvement in our ability to discern individual action potentials in our optical mapping data without post-processing for noise removal (e.g. signal averaging) as a result of this increased illumination light intensity.

Although we have improved the signal quality in our data, there are still pixels where the noise masks the action potentials. The variability in pixel signal quality may stem from several factors, such as a) noisy pixels at the edge of the preparation b) difficulty recording in the inter-atrial space due to the presence of fatty tissue and vessels, c) uneven dye uptake, d) other noise sources associated with a CCD device [11] and e) relatively low illumination light, even despite our system improvements in this area. These noisy pixels in turn decrease the overall quality of the optical mapping video, making it difficult to perform a detailed analysis of the pattern of electrical activity throughout the tissue. However, the quality of the optical mapping recordings is sufficient for general qualitative observations regarding the propagation of electrical signals during arrhythmic activity.

In past work, signal averaging has been used to increase the signal-to-noise ratio in the optically recorded signals to an acceptable level for the study of action potential durations, conduction velocities and overall activation/conduction patterns [8]. However, in the case of the arrhythmic activity, signal averaging is no longer an acceptable noise-removal technique because the periodicity of the activity cannot be guaranteed (even given the apparent regularity of our recorded arrhythmias). Clearly, more work is needed in developing alternative methods for post-processing of the optical mapping videos for noise removal. With cleaner AP signals and optical mapping videos, it will be possible to further investigate the properties and patterns of electrical activity in the isolated mouse atria during the induced arrhythmias.

V. CONCLUSIONS

This preliminary work has shown that our optical mapping system provides an adequate means for visualizing the basic properties of arrhythmias induced in the isolated mouse atrial preparation. Without any additional post-processing for noise removal, it is possible to distinguish individual optically recorded action potentials and to make some general observations regarding the propagation of electrical signals during the arrhythmic activity. These initial results support future endeavours in studying the mechanisms of atrial arrhythmias in the mouse heart with the isolated atrial preparation. Future work will involve investigating post-processing techniques for improving the optical mapping signal quality, in order to have a more complete view of the propagation of electrical activity during arrhythmic behaviour. On the experimental side, future work will include investigating the reproducibility of arrhythmia induction, examining other arrhythmia induction protocols and applying these techniques to study atrial arrhythmias in transgenic mouse models.

REFERENCES

[1] T. Thom, *et al.*, "Heart disease and stroke statistics–2006 update: A report from the American Heart Association statistics committee and stroke statistics subcommittee," *Circulation*, vol. 113, no. 6, pp. e85–e151, 2006.

[2] S. Nattel, "New ideas about atrial fibrillation 50 years on," *Nature*, vol. 415, no. 6868, pp. 219–226, 2002.

[3] I. R. Efimov, V. P. Nikolski, and G. Salama, "Optical imaging of the heart," *Circ.Res.*, vol. 95, no. 1, pp. 21–33, 2004.

[4] A. C. Skanes, *et al.*, "Spatiotemporal periodicity during atrial fibrillation in the isolated sheep heart," *Circulation*, vol. 98, no. 12, pp. 1236–1248, 1998.

[5] S. Verheule, *et al.*, "Direction-dependent conduction abnormalities in a canine model of atrial fibrillation due to chronic atrial dilatation," *Am. J. Physiol. Heart Circ. Physiol.*, vol. 287, no. 2, pp. H634–H644, 2004.

[6] H. Wakimoto, *et al.*, "Induction of atrial tachycardia and fibrillation in the mouse heart," *Cardiovasc.Res.*, vol. 50, no. 3, pp. 463–473, 2001.

[7] P. Kovoor, *et al.*, "Evaluation of the role of I(KACh) in atrial fibrillation using a mouse knockout model," *J. Am. Coll. Cardiol.*, vol. 37, no. 8, pp. 2136–2143, 2001.

[8] A. Nygren, A. E. Lomax, and W. R. Giles, "Heterogeneity of action potential durations in isolated mouse left and right atria recorded using voltage-sensitive dye mapping," *Am. J. Physiol. Heart Circ. Physiol.*, vol. 287, no. 6, pp. H2634–H2643, 2004.

[9] P. Schaffer, *et al.*, "Di-4-ANEPPS causes photodynamic damage to isolated cardiomyocytes," *Pflugers Arch.*, vol. 426, no. 6, pp. 548–551, 1994.

[10] R. B. Schuessler, *et al.*, "Cholinergically mediated tachyarrhythmias induced by a single extrastimulus in the isolated canine right atrium," *Circ.Res.*, vol. 71, no. 5, pp. 1254–1267, 1992.

[11] G. C. Holst, *CCD Arrays, Cameras, and Displays*. JCD Publishing & SPIE Optical Engineering Press, 1998.

[12] F. X. Witkowski, *et al.*, "A method for visualization of ventricular fibrillation: Design of a cooled fiberoptically coupled image intensified CCD data acquisition system incorporating wavelet shrinkage based adaptive filtering," *Chaos*, vol. 8, no. 1, pp. 94–102, 1998.